PROCEEDINGS OF SCIENCE

Antihydrogen annihilation detection: the ALPHA-g radial TPC

Andrea Capra[a,*] **for the ALPHA collaboration**

[a] *TRIUMF,*
Wesbrook Mall 4004, Vancouver BC, Canada

E-mail: `acapra@triumf.ca`

The recent measurement of the antihydrogen terrestrial gravitational acceleration with the ALPHA-g apparatus at CERN relies upon the detection of the annihilation of the anti-atoms that are released from their magnetic confinement and that move under the influence of gravity. The ALPHA-g magnetic trap is surrounded by a Time Projection Chamber designed to identify the annihilation products and to reconstruct the annihilation position. The TPC is called "radial", or rTPC, because the drift field is perpendicular to the trap axis and, therefore, to the magnetic field of the external field. The design, construction and commissioning of this detector are described in the following.

International Conference on Exotic Atoms and Related Topics and Conference on Low Energy Antiprotons (EXA-LEAP2024)
26-30 August 2024
Austrian Academy of Sciences, Vienna.

---

[*] Speaker

https://pos.sissa.it/

PoS(EXA-LEAP2024)063

1. Introduction

Antihydrogen ($\overline{\mathrm{H}}$) annihilation imaging is an essential tool for the ALPHA physics program at the CERN Antimatter Factory. The ALPHA collaboration recently measured the terrestrial gravitational acceleration of $\overline{\mathrm{H}}$ with the ALPHA-g apparatus [1]. A position sensitive detector is used to reconstruct the $\overline{\mathrm{H}}$ annihilation position in the ALPHA experiment and it serves as the main spectroscopic signal. The gravity measurement campaign of ALPHA-g depends as well on the detection of the $\overline{\mathrm{H}}$ annihilation position. The ALPHA-g $\overline{\mathrm{H}}$ magnetic traps span more 2 m in length and, given this size, an annihilation detector that employs a gas as the active medium ensures high acceptance, while remaining cost effective. The gas detector technology of choice of ALPHA-g is a Time Projection Chamber [2], which minimizes the number of sensing wires required to determine the trajectory of a charge particle. The complex magnetic environment of the ALPHA-g apparatus, including the fringing field effects of the external 1 T solenoid, lead to the choice of a radial drift chamber, where the electric field is orthogonal to the solenoidal magnetic field, which coincides with the $\overline{\mathrm{H}}$ magnetic trap axis, as well as, the detector axis. Since $\boldsymbol{E}_{\mathrm{drift}} \perp \boldsymbol{B}_{\mathrm{solenoid}}$, the detector is called "radial", hence *rTPC*, see Fig. 3a. In addition to the rTPC, the ALPHA-g apparatus is endowed with a barrel scintillator detector, or BSC, that surrounds the rTPC, inside the solenoid. This detector is used to enhance the cosmic ray rejection capability (the main source of background signals to the detection of $\overline{\mathrm{H}}$ annihilation) with a Time-Of-Flight method, combined with Machine Learning algorithm [3].

Figure 1: The ALPHA-g rTPC moments before being installed into the ALPHA-g apparatus

2. Mechanical and Electrical Design

The active length of the rTPC is $L = 2,304$ mm, that is the length of the $n_{\mathrm{AW}} = 256$ sensing or *anode* wires. The anode wires are strung between the top and bottom end-plates, attached to the inner cylinder that is the cathode. The diameter of the inner cathode is 20 cm. Finally, the active volume of gas is enclosed at the outer radius $r_{\mathrm{pad}} = 19$ cm by a set of segmented cathodic electrode, called the *pads*. There are $n_{\mathrm{row}} = 576$ pads in the direction parallel to the rTPC axis and $n_{\mathrm{col}} = 32$, for a total of $n_{\mathrm{row}} \times n_{\mathrm{col}} = n_{\mathrm{pad}} = 18,432$, see Fig. 2a.

The gas volume is divided in two regions by the 256 field wires (see Fig. 3a), located at 17.4 cm from the rTPC axis. The innermost region is called the *drift region* and its radial extent is

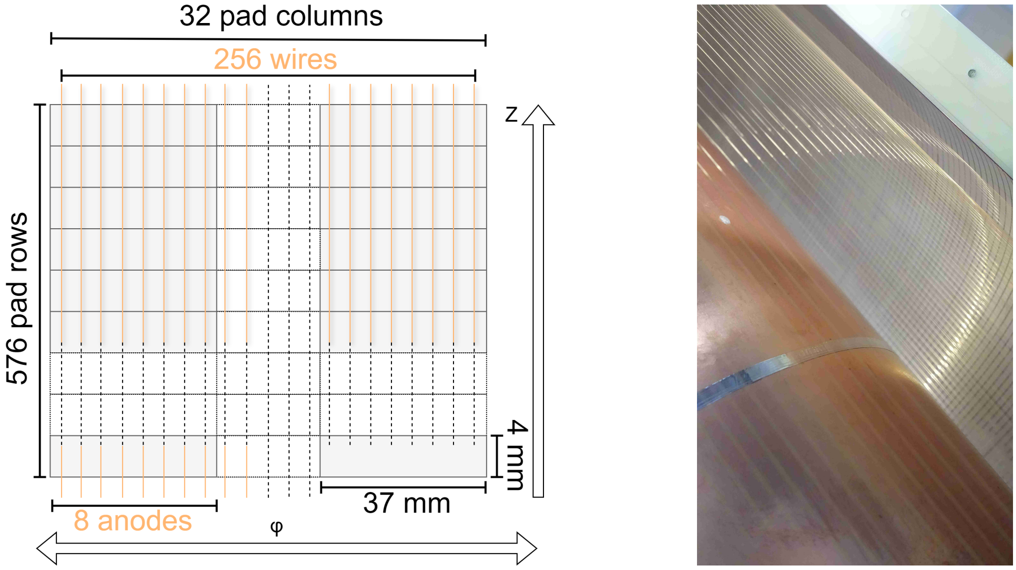

(a) Schematic view of the distances and sizes of the rTPC electrodes, as it would appear if the outer cylinder is unravelled. For clarity, only few anode wires and pads are shown in this projection in the $\varphi - z$ plane.

(b) Photograph of the rTPC with only one half of the outer cathode assembled. The inner cathode, the field wires, the anode wires and the pads are all visible in the picture.

Figure 2

therefore 7.4 cm. The cylindrical shell comprised between the field wires and the pads is dubbed *amplification region*, and is dedicated to the amplification, via charge avalanche multiplication, of the ionization produced by the charged particles interacting in the drift region. The anode wires occupy the geometric centre of the amplification region at $r_{\mathrm{AW}} = 18.2$ cm from the rTPC axis, that is, separated by 8 mm (radially) both from the field wires and the pads. Such an arrangement can be appreciated in Fig. 2b. The separation of the active volume into two distinct regions allows the users to control the drift field independently from the charge multiplication field.

The field wires diameter (75 μm) and tension (120 g), as well as, the anode wires tension, (40 g) are determined from electrostatic calculation based on [4], taking into account that the anode wires diameter is inversely proportional to the gas gain. The diameter of the anode wires was chosen to be 30 μm, following the studies performed with a single wire proportional tube, filled with the same gas mixture as in the rTPC.

The anode wires pitch $2\pi r_{\mathrm{AW}}/n_{\mathrm{AW}} = 4$ mm is chosen using Monte Carlo simulation, based on Geant4 [5], to optimize the radial resolution, which is known to be limited by the multiple Coulomb scattering due to the presence of high atomic number materials between the $\overline{\mathrm{H}}$ annihilation location and the detector. The pad pitch $L/n_{\mathrm{row}} = 4$ mm along the rTPC axis is similarly determined. On the contrary, the pitch along the azimuthal direction φ is $2\pi r_{\mathrm{pad}}/n_{\mathrm{col}} = 37$ mm to reduce the number of readout channels, while maintaining the angular resolution by virtue of the anode wires spacing.

The drift (electric) field is about $\approx$ 1 kV/cm, see Fig. 3b. This is achieved by biasing the cathode at -4 kV, while keeping the field wires at -101 V. The anode wires are nominally at 3.2kV, which produce an gas multiplication gain greater than 10^4.

The gas in the chamber is a mixture of argon and carbon dioxide. Since the rTPC is immersed in a 1 T magnetic field, the proportions are such that the drift velocity is $\approx$ 20 μm/ns and the

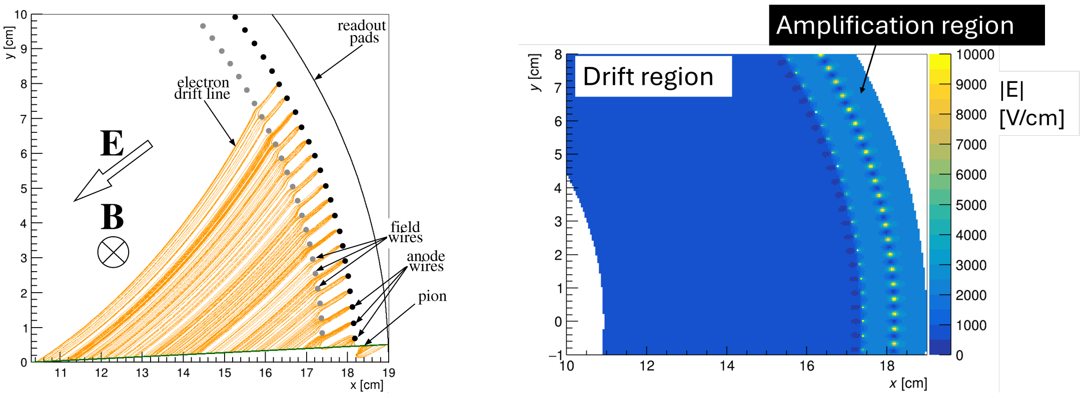

(a) Cross-sectional view of a quarter of the rPTC, which shows the simulated path of a charged pion (green) ionizing the gas in the rTPC. Orange lines show the drift of electrons in the magnetic and electric fields [6]. The diameter of the field and anode wires is greatly exaggerated.

(b) Heatmap showing the value of the electric field imposed in the active volume of the rTPC when the electrodes are set to their nominal voltage (see text).

Figure 3

deflection of the drifting charges due to the Lorentz force is ≈ 11°, which corresponds to roughly the size of a pad along the azimuth.

3. Frontend Electronics

The readout of the anode wires is performed with custom electronics capacitively coupled to the wires. Each readout card, called Anode Wire Board, or AWB, is connected to 16 wires. There are, therefore, 16 AWBs in the rTPC, connected to the top end of the end anode wires.

Given the large number of pads, the signal induced by the electron avalanche is digitized on the detector by means of 64 electronic modules, called Pad-Wing Boards, or PWBs. They are arranged in eight columns, and each column comprises eight PWBs. Each board is composed of two *wings* on each side of a central body, and connected to it via a flexible kapton cable. This design is devised in order to fit each module to the cylindrical shape of the rTPC. Each board has four AFTER ASICS [7], which are switching capacitor arrays, connected to 72 pads. There are two AFTER chips per wing, connected to a 14 bits 62.5MS/s ADC. The central body of the module hosts an Altera Cyclone 5 FPGA, which coordinates the readout of the pads signal, performs data suppression and sends the digital data to the data acquisition system via 1Gps optical link. The PWBs installed on the rTPC are visible in Fig. 1. Given that each board required about 15 W of power, the PWBs are water cooled by means of copper piping that run along the rTPC length in eight cooling loops (one per column).

The raw signals from the anode wires and the pads are collected are processed by the data acquisition system.

4. Data Acquisition

The Data Acquisition System, or DAQ, is network based. The data flow through a 96 ports Juniper switch at a maximum bandwidth of 1 Gps, while the link between the switch and the central

DAQ server is 10 Gps. Figure 4 provides an overview of the essential elements of the ALPHA-g DAQ, including the "on detector" frontend electronics, described in the previous section.

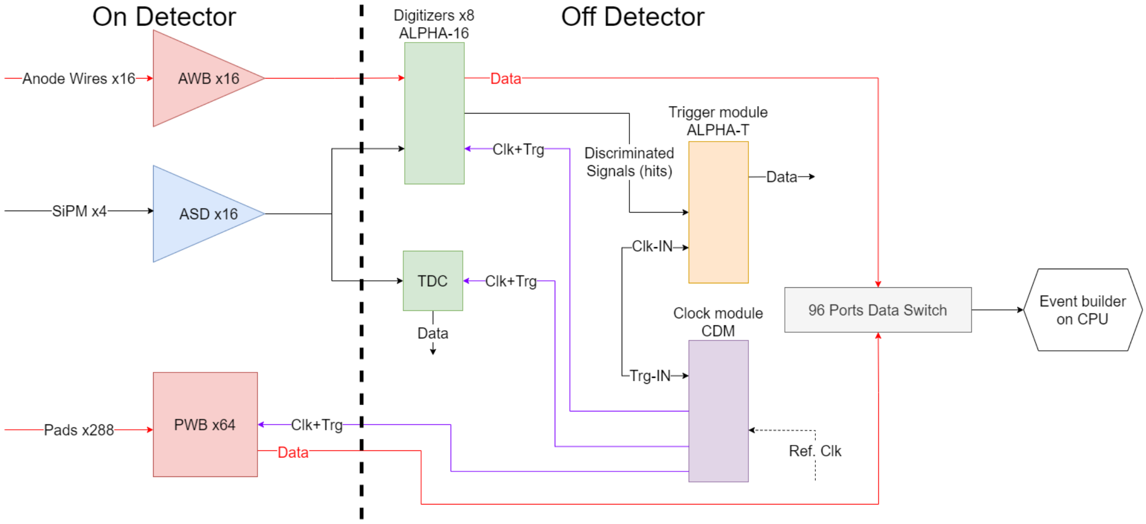

Figure 4: Vertical slice of the rTPC data acquisition system with data flow. Except for the data switch, manufactured by Juniter and the GSI TRB3 TDC, all the units depicted in this sketch have been developed at TRIUMF. The complete system has eight ALPHA-16 digitizers and two clock modules CDM.

The anode wires analog signals are digitized by eight custom digitizers, called ALPHA-16. Each digitizer has a frontend "mezzanine" card, or FMC, that accepts the analog signals from two AWBs. The ALPHA-16 are used also to digitize the Barrel Scintillator signals, which are connected to the back pane of the VME crate. The hearts of the FMC are two 16 bits 62.5 MS/s ADC. The digitized waveforms go into a digital discriminators, that is a function provided by the custom firwmare running on the Altera Cyclone 5 FPGA on the ALPHA-16. This FPGA also performs data suppression and coordinates the transmission of the data packets via 1Gps optical link.

Based on the discriminated wire signals, a custom trigger module, called ALPHA-T, computes a trigger signal based on the multiplicity and the topology of "hits" on the anode wires, as shown in Tab 1. The rTCP *self-trigger* signal from the ALPHA-T is distributed through the Clock Distribution Modules, or CDM, to the ALPHA-16, the PWBs and the TDC[1]. There are two CDMs, synchronized on a master 62.5 MHz clock, which is generated either using the internal 10 MHz oscillator, or an external 10 MHz "atomic" clock. The CDMs are responsible for synchronizing the readout of the rTPC and BSC data.

Typical trigger rates due to cosmic rays and other activities in the experimental hall are about 70 Hz, when the thresholds of the anode wires discriminator are set just above the electronic noise level. The readout rate is limited to 500 events per second, due to the read time of the AFTER ASIC.

Because all the rTPC (and BSC) data come from different sources, the task of matching the raw databy timestamp to create physics events is delegated to the *event builder*, or EVB. The EVB is a multithreaded program that runs on the main DAQ server, and is built as a MIDAS frontend [9, 10].

---

[1] The Time to Digital Converter model TRB3 [8], manufactured by GSI, is used only for the BSC to provide the best time resolution for the Time-Of-Flight measurements.

.	.	.	.	.	.	.	.	.	.	.	.	.	.	.	.	trivial
X	.	.	.	.	.	.	.	.	.	.	.	.	.	.	.	no trigger
X	X	.	.	.	.	.	.	.	.	.	.	.	.	.	.	no trigger
X	.	X	.	.	.	.	.	.	.	.	.	.	.	.	.	trigger!
X	.	.	X	.	.	.	.	.	.	.	.	.	.	.	.	trigger!
X	X	.	X	.	.	.	.	.	.	.	.	.	.	.	.	trigger!
etc.																

Table 1: The trigger logic is based on a Memory Lookup Table, or MLU, which is an arbitrary logical function. The trigger signal is generated when two or more AWBs with a gap have a hit, with the condition that two or more adjacent AWB (no gap) count as one. Each "." represent an AWB without a hit, while the "X" represents one with a hit. It is worth noting that the first three rows are not actually loaded into the trigger module, but are shown here just for clarity.

Each thread executes a specific function: receive data packets, decode the packets, build the event, and send it to local memory buffer. The events are written to disk by the MIDAS dedicated routine and analyzed in real-time by a dedicated "reconstruction" software.

5. Annihilation Vertex Reconstruction

Each event readout by the DAQ must be analyzed to determine whether it is due to $\overline{\mathrm{H}}$ annihilating with ordinary matter. The hallmark of an annihilation in the ALPHA-g trap is its three-dimensional position, referred as the *vertex*. This kind of analysis is often referred as "the reconstruction" and, in the case of the rTPC proceeds, through the following steps: 1) analysis of the anode wires and pad waveforms; 2) charged pion tracks identification; 3) determination of the point where the identified tracks pass closest to each other.

When a charge pion deposits its energy in the gas, electrons are freed and drift radially towards an anode wire. An anode waveform contain both the information of the avalanche multiplication initiated in its vicinity, as well as the ones due to the electron multiplication that occurred on neighbouring wires. In order to extract accurate position information, only the former must be retained. The correct electron arrival time (drift time) is obtained by employing the signal template as a digital filter. The number of pads involved in each avalanche is greater than one, thus pads grouping is necessary. The centroid of the distribution of the induced charge on the pads defines the location of the avalanche along the rTPC axis. The drift time is converted to the radial coordinate by means of tabulated *space-time relation*. The three-dimensional position of the interaction of a charged particle with the gas, a *spacepoint*, is obtained by matching the wires and pads by drift time using a *k-d tree* algorithm [11]. Since the drift occurs in a magnetic field, the effect of the Lorentz force is taken into account when determining the azimuthal coordinate of the spacepoint.

The spacepoints are combined into tracks based on their relative distance, since closer points are most likely part of the same charged pion track. Each track is seeded from a spacepoint chosen near the outer edge of the fiducial volume. Moving inwards, the closest spacepoint is added to the track. Each spacepoint added this way is then treated as a seed spacepoint. This repeats until either there are no spacepoints within a threshold distance, or the inner cathode is reached. Each spacepoint added this way is then treated as a seed spacepoint, and more spacepoints are added to the track. A three-dimensional helix function is fit to the array of spacepoints using the least-squares method. The canonical parameters of the helix and their uncertainties are found by minimizing the three-dimensional distance from each spacepoint in the track to the helix function.

The last step consists in determining the vertex location from the helix analytical functions. The first guess of the vertex position is made using the pair of helices that pass closest to each other, and taking the midpoint along the segment that joins them at their closest approach. This estimate is improved by minimizing the distance between the helix pair and the first vertex position, weighted by their errors from previous best-fit. In the final step, each additional helix is considered in the same minimization procedure. New helices are included only if the overall weighted distance remains below an optimal value.

6. Background Rejection

Once a vertex is found, it does not necessarily mean that it is the result of $\overline{\mathrm{H}}$ annihilation. Cosmic rays are an obvious alternative explanation. Since non-physical vertices due to cosmic rays occur at a rate of about 6 Hz, common background rejection techniques are employed to get rid of unwanted events. The most powerful tool currently used in ALPHA-g is the Boosted Decision Tree (BDT) algorithm [12]. This is a classification algorithm with two classes: signal and background. It is trained using real data [13]: the signal sample is derived from the production of $\overline{\mathrm{H}}$, where untrappable $\overline{\mathrm{H}}$ triggers the detector at high rate in a short period of time, while the background sample is obtained by acquiring data without antiparticles in the ALPHA-g apparatus. When applying the classifier on a test sample of annihilation events, 63% of those events are retained, while on a background sample the *false positive rate* is maintained to ≈ 0.12 Hz, as shown in Fig. 5.

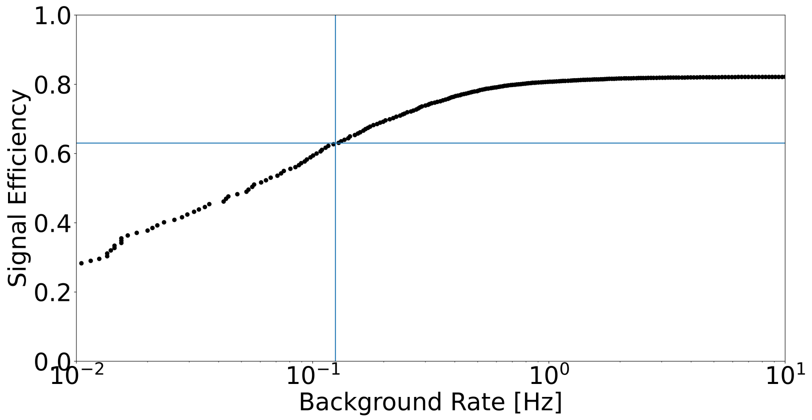

Figure 5: BDT classifier performance, as a function of the classifier cut value (black dots). The false positive rate is obtained by counting how many vertices survive the selection in the (pure) background test sample. The signal efficiency is determined from the ratio of the number of vertices that pass the cut to the total number of events contained in the signal test sample. The blue lines indicate the choice made for [1].

7. Performance

The performance of the rTPC, and of its reconstruction software, were first assessed using a Monte Carlo simulation, based on Geant4 that used drift and charge amplification data obtained with Garfield++, and data-driven signals template to generate realistic waveforms for both the anode wires and the pads. The reconstruction of the simulated annhilation, which includes the trigger logic described in Tab. 1, yields a vertex for 83% of the total number of generated events. The resolution along the rTPC axis (vertical), measured as width of the distribution of the distance between the true annihilation position and the reconstructed one, is 14 mm, which is sufficient to carry out the ALPHA-g physics program.

Additional tests on bare antiproton annihilation data are shown in Fig. 6a, where the antiproton plasma was confined simultaneously in four different electrodes of the ALPHA-g Penning trap. After the positions of the centres of the four distributions are extracted from a common function, a least square fit to a straight line is performed, which yields an offset between the expected and measured position of the plasma inferior to 5 mm (see Fig. 6b). This value is well within the tolerance of the rTPC-Penning trap alignment, indicating the tracking detector positively identifies the location of the antiproton annihilation in the real setup.

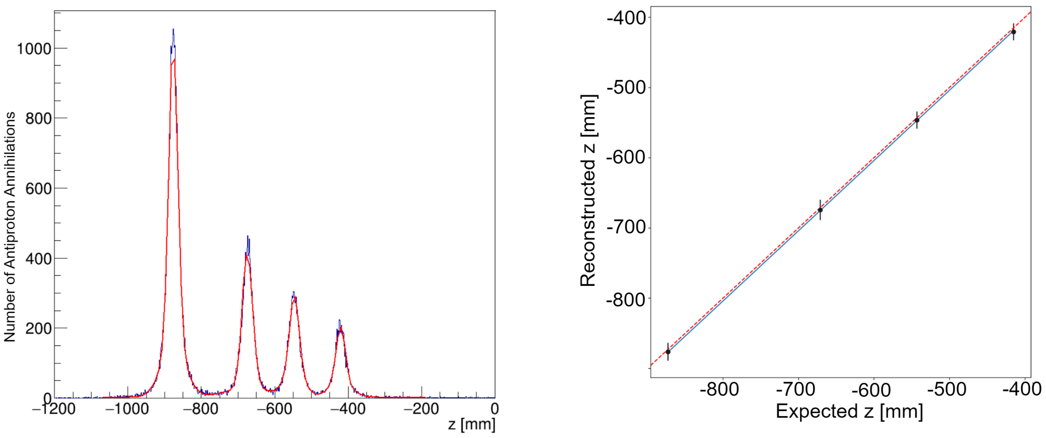

(a) Reconstruction of antiproton annihilation, the antiprotons are held in four different electrodes simultaneously. The horizontal axis represents the coordinate along the rTPC axis z, whose 0 is the geometrical centre of the detector. The vertical axis is the count of antiproton annihilation, after background suppression.

(b) Expected (x-axis) vs. reconstructed (y-axis) position of the electrode holding the antiproton plasma. The black dots indicate the centres of the distribution on the left, overlaid with a straight line fit in light blue. This shows a minimal and well-understood offset compared to the dashed red line, which indicates no offset between the expected and the measured position of the plasma.

Figure 6

8. Conclusions

The measurement of $\overline{\mathrm{H}}$ gravity undertaken by the ALPHA collaboration requires the detection of the $\overline{\mathrm{H}}$ annihilation, and the determination of its position. The rTPC, designed and built at TRIUMF (Vancouver, Canada), is in operation in the ALPHA-g experiment and is successfully accomplishing that task, leading to the first observation of the $\overline{\mathrm{H}}$ free-fall. The electronics and DAQ, presented in this paper, perform as designed. The reconstruction algorithms successfully find the annihilation location, and are always being improved. For example, a novel project is underway to deploy a deep learning method to perform vertex reconstruction.

Acknowledgments

This work was supported by NSERC, NRC/TRIUMF, CFI. We thank P. A. Amaudruz, D. Bishop, J. Blando, I. Carli, S. Chan, M. Constable, D. Duque, W. Frazer, L. Golino, R. Henderson, P. Lu, L. Kurchaninov, T. Lindner, R. Maharaj, L. Martin, J. T. McKenna, A. Miller, K. Olchanski, K. Ong, L. Paulson, F. Retiere, B. Shaw G. Smith, and P. Vincent for their work on the ALPHA-g detectors, the data acquisition system, and the online and offline software.

References

[1] E.K. Anderson et al. Observation of the effect of gravity on the motion of antimatter. *Nature*, 621(7980):716–722, 2023.

[2] A. Capra et al. Design of a Radial TPC for Antihydrogen Gravity Measurement with ALPHA-g. In *Proceedings of the 12th International Conference on Low Energy Antiproton Physics (LEAP2016)*, page 011015, 2017.

[3] G. Smith. Background Rejection for the ALPHA-g Anti-Hydrogen Detectors. In *Proceedings of International Conference on Exotic Atoms and Related Topics and Conference on Low Energy Antiprotons*, PoS (EXA-LEAP2024)0xx, 2024.

[4] R. Veenhof. Simulation of gaseous detectors. `garfield.web.cern.ch/garfield`.

[5] S. Agostinelli et al. Geant4—a simulation toolkit. *Nuclear Instruments and Methods in Physics Research Section A: Accelerators, Spectrometers, Detectors and Associated Equipment*, 506(3):250–303, 2003.

[6] H. Schindler and R. Veenhof. Garfield++: simulation of ionisation based tracking detectors. `garfieldpp.web.cern.ch/garfieldpp`.

[7] P. Baron et al. AFTER, an ASIC for the Readout of the Large T2K Time Projection Chambers. *IEEE Transactions on Nuclear Science*, 55(3):1744–1752, 2008.

[8] A. Neiser et al. TRB3: a 264 channel high precision TDC platform and its applications. *Journal of Instrumentation*, 8(12):C12043, 2013.

[9] S. Ritt, P. Amaudruz, and K. Olchanski. The MIDAS data acquisition system. In *Proc. IEEE 10th Real Time Conference*, pages 309–312, 1997.

[10] S. Ritt, P. Amaudruz, and K. Olchanski. MIDAS, Data Acquisition System. `daq00.triumf.ca/MidasWiki/index.php/Main_Page`.

[11] Jon Louis Bentley. Multidimensional binary search trees used for associative searching. *Commun. ACM*, 18(9):509–517, September 1975.

[12] A. Hoecker et al. TMVA - Toolkit for Multivariate Data Analysis, 2009.

[13] Capra, A. (ALPHA Collaboration). Machine learning for antihydrogen detection at ALPHA. In *Journal of Physics: Conference Series*, volume 4, page 042007. IOP Publishing, 2018.